JCI The Journal of Clinical Investigation

Relationship between calcium loading and impaired energy metabolism during Na+, K+ pump inhibition and metabolic inhibition in cultured neonatal rat cardiac myocytes.

A C Morris, … , J T Willerson, L M Buja

J Clin Invest. 1989;83(6):1876-1887. https://doi.org/10.1172/JCI114094.

Research Article

This study tested the hypothesis that the initiating mechanism is a major determinant of the response to calcium (Ca) accumulation in myocardium. Cultured neonatal rat ventriculocytes were exposed to Na+, K+ pump inhibition with 1 mM ouabain and metabolic inhibition with 20 mM 2-deoxy-D-glucose and 1 mM cyanide (DOG-CN) for up to 2 h. Microspectrofluorometry of myocytes loaded with fura-2 showed that ouabain resulted in a relatively rapid increase in [Ca2+]i up to 2-3 microM (two to threefold above peak systolic level) and that DOG-CN produced an initial decrease and then a relatively slow increase in [Ca2+]i up to peak systolic level. Electron probe x-ray microanalysis (EPMA) showed prominent increases in Na and Ca and decreases in K and Mg in cytoplasm and mitochondria with both interventions, although the increases in Ca were greater with ouabain than DOG-CN. ATP was reduced by 58% after 1 and 2 h of ouabain and by 70 and 90% after 1 and 2 h of DOG-CN, respectively. Thus, ouabain produced greater calcium accumulation and less ATP reduction than DOG-CN. Upon return to normal medium for 30 min, myocytes showed recovery of most electrolyte alterations and resumption of normal Ca2+ transients after 1 h exposure to either ouabain or DOG-CN; however, recovery was less after 2 h of either treatment, with elevated [Ca2+]i maintained in […]

Relationship between Calcium Loading and Impaired Energy Metabolism during Na^+, K^+ Pump Inhibition and Metabolic Inhibition in Cultured Neonatal Rat Cardiac Myocytes

Alan C. Morris, Herbert K. Hagler, James T. Willerson, and L. Maximilian Buja
With the technical assistance of **Dennis Bellotto, Donna Buja, and Bruce Ziman**
Departments of Pathology and Internal Medicine (Cardiology Division), The University of Texas Southwestern Medical Center at Dallas, Dallas, Texas 75235-9072

Abstract

This study tested the hypothesis that the initiating mechanism is a major determinant of the response to calcium (Ca) accumulation in myocardium. Cultured neonatal rat ventriculocytes were exposed to Na^+, K^+ pump inhibition with 1 mM ouabain and metabolic inhibition with 20 mM 2-deoxy-D-glucose and 1 mM cyanide (DOG-CN) for up to 2 h. Microspectrofluorometry of myocytes loaded with fura-2 showed that ouabain resulted in a relatively rapid increase in $[Ca^{2+}]_i$ up to 2–3 μM (two to threefold above peak systolic level) and that DOG-CN produced an initial decrease and then a relatively slow increase in $[Ca^{2+}]_i$ up to peak systolic level. Electron probe x-ray microanalysis (EPMA) showed prominent increases in Na and Ca and decreases in K and Mg in cytoplasm and mitochondria with both interventions, although the increases in Ca were greater with ouabain than DOG-CN. ATP was reduced by 58% after 1 and 2 h of ouabain and by 70 and 90% after 1 and 2 h of DOG-CN, respectively. Thus, ouabain produced greater calcium accumulation and less ATP reduction than DOG-CN. Upon return to normal medium for 30 min, myocytes showed recovery of most electrolyte alterations and resumption of normal Ca^{2+} transients after 1 h exposure to either ouabain or DOG-CN; however, recovery was less after 2 h of either treatment, with elevated $[Ca^{2+}]_i$ maintained in many myocytes. We conclude that the severity of myocyte injury is influenced by the magnitude and duration of both ATP reduction and calcium accumulation.

Introduction

Myocardial ischemia leads to impaired energy metabolism, membrane dysfunction, and altered calcium (Ca) homeostasis (1–10). These metabolic and pathophysiological alterations are thought to lead to the progression of irreversible injury; however, the exact role of each of these factors is still unclear. Specifically, some evidence suggests that a marked increase in cytosolic Ca^{2+} in ischemic or hypoxic myocytes can result in irreversible myocardial injury, whereas other observations suggest that alterations of energy metabolism may be of primary importance in the pathogenesis of irreversible myocardial injury (1–6).

Studies by Murphy et al. have indicated that the response of cardiac myocytes to calcium overloading is influenced by the mechanism of initiation of calcium accumulation (11, 12). Specifically, these workers reported that cultured chick ventricular myocytes developed less severe acute injury when the myocytes became calcium loaded after Na^+, K^+ pump inhibition than after metabolic inhibition. In the same cellular model, however, Ishida et al. found that Na^+, K^+ pump inhibition produced more severe calcium accumulation than did metabolic inhibition, and that very profound metabolic inhibition was required to approximate the severity of cell injury induced by Na^+, K^+ pump inhibition (13). These findings have raised questions related to the dynamics of changes in calcium homeostasis, including free and total calcium pools, the relationship of changes in calcium and high-energy phosphate metabolism, and the potential for recovery after various perturbations affecting the intracellular calcium level.

To study various factors that may contribute to irreversible myocardial injury, we have used an isolated neonatal rat ventricular myocyte model (8–10). In the present study, altered calcium homeostasis was induced by: (*a*) inhibition of the Na^+, K^+ pump by exposure to 1 mM ouabain, with secondary activation of Na^+-Ca^+ exchange (14–16), and (*b*) by exposure of the myocytes to the metabolic inhibitors, 2-deoxy-D-glucose (DOG)[1] and sodium cyanide (CN) (17). Dynamic intracellular Ca^{2+} concentrations ($[Ca^{2+}]_i$) were measured with the fluorescent indicator, fura-2 (18), using quantitative microspectrofluorometry. The analytical electron microscope technique of electron probe x-ray microanalysis (EPMA) was used to measure the total content of calcium and other elements in subcellular compartments of individual myocytes (10). These approaches have provided quantitative data regarding changes in free and total calcium under the same experimental conditions. In addition, alterations in calcium homeostasis were related to changes in high-energy phosphate metabolism, and specifically ATP levels, both during exposure to interventions and in the recovery period.

This study was performed to test the hypotheses that: (*a*) the dynamics of changes in cellular calcium homeostasis, including free and total calcium pools, differ in response to the mechanism of calcium loading; (*b*) the amount, distribution,

Portions of this work were reported in preliminary form in the following abstracts: 1987. *Fed. Proc.* 46:1095 and 1988. *FASEB (Fed. Am. Soc. Exp. Biol.) J.* 2:A1157.

Address reprint requests to Dr. L. Maximilian Buja, Pathology Department, University of Texas Southwestern Medical Center at Dallas, 5323 Harry Hines Blvd., Dallas, TX 75235-9072.

Received for publication 1 June 1987 and in revised form 18 January 1989.

J. Clin. Invest.

0021-9738/89/06/1876/12 $2.00
Volume 83, June 1989, 1876–1887

1. *Abbreviations used in this paper:* CN, cyanide; DOG, 2-deoxy-D-glucose; EPMA, electron probe x-ray microanalysis; LDH, lactic dehydrogenase; R, recovery; STEM, scanning transmission electron microscopy.

and duration of calcium overloading influences the severity of cell injury; and (*c*) the status of energy metabolism associated with calcium overloading is an important determinant of the capability of calcium-overloaded myocytes to compensate for homostatic alterations. The results indicate that the mechanism of calcium accumulation, as well as the magnitude and duration of altered calcium homeostasis, and associated changes in ATP levels, influence the potential for recovery from calcium loading in cultured neonatal rat ventricular myocytes.

Methods

Isolated myocyte model. Ventricular myocytes from the hearts of 2–3-d-old rats were cultured using previously described methods (10). The myocardial cells were dispersed by a series of 20-min incubations at 37°C in a nominally calcium-free, Hepes-buffered salt solution containing pancreatin (60 mg/100 ml) (Gibco Laboratories, Grand Island, NY) and type II collagenase (6,000–6,400 U/100 ml) (Cooper Biomedical, Freehold, NJ). Myocyte enrichment was achieved by the use of a discontinuous step gradient of Percoll (Pharmacia Fine Chemicals, Uppsala, Sweden) (19). The cells were plated at a density of 1.5–1.8 million per 60-mm culture dish in culture medium (Gibco Laboratories) consisting of 68% DME, 17% medium 199 with Earle's salts, 10% horse serum, 5% FCS and antibiotics (10,000 U/ml penicillin, 10 mg/ml streptomycin). The calcium concentration was 1.8 mM. Cultures were exposed to 7% CO_2 and maintained with the pH of the medium at 7.3 and at 37°C in a tissue culture incubator.

Experimental protocols. Experiments were performed on 3- or 4-d-old cultures that typically were composed of ~ 85% beating myocytes. Control cultures were incubated in serum-free medium 199 or in control Tyrode's solution consisting of (in millimolar): NaCl, 118; NaH_2PO_4, 0.8; $MgSO_4$, 0.8; $NaHCO_3$, 26.2; KCl, 5.4; glucose 5.6; and $CaCl_2$, 1.8. Solutions were prepared with cell culture-grade reagents (Sigma Chemical Co., St. Louis, MO). Na^+, K^+ pump inhibition was initiated by incubation in serum-free medium 199 or Tyrode's solution containing 1 mM ouabain. The concentration of ouabain was chosen on the basis of preliminary dose-response experiments that showed that 1 mM ouabain gave a reproducible and relatively rapid contracture. For metabolic inhibition, 20 mM DOG and 1 mM NaCN were added to serum-free medium 199 or Tyrode's solution. This dose of metabolic inhibitor was chosen based on previous work establishing the general response of cardiac myocytes to metabolic inhibition (8–10). In experiments involving treatment of myocytes in culture dishes with DOG-CN for 2 h, treatment medium was changed at the end of 1 h to provide a second dose of DOG-CN, thus compensating for possible loss of CN due to formation of CN gas. Microspectrofluorometric experiments involved continuous superfusion with DOG-CN. Exposure to DOG and CN was performed in the presence and absence of glucose in the medium without important effect on the results. In recovery experiments, the control or test media were replaced with normal medium 199 containing 1.8 mM Ca^{2+}. Experiments were performed with three culture plates in each group.

Measurement of ionic calcium transients. For experiments in which dynamic changes in ionic calcium were measured by quantitative microspectrofluorometry, myocytes were grown on laminin-coated, 25-mm-diam glass coverslips. The coverslips were treated with laminin (20 μg/ml medium) (Collaborative Research, Lexington, MA) for 1 h before seeding with myocytes. After 3 or 4 d in culture, the myocytes were treated with phenol red–free medium 199 containing 1% FCS and 3.0 μM fura 2/AM (Calbiochem-Behring Corp., La Jolla, CA) for 30 min at 37°C. After the fura 2/AM loading period, the cells were equilibrated in fura-free medium 199 for 30–60 min, at which time the experiments were performed.

The coverslips were mounted in Sykes-Moore chambers (Belco Glass Co., Vinewood, NJ) and examined with a Nikon Diaphot microscope equipped with UV light optics, a heated stage, and a perfusion pump. Calcium transients associated with spontaneous contractions of the myocytes were measured using alternating 340 and 380 nM excitation produced by a microspectrofluorometer (Fluoroplex 1000; Tracor Northern, Middleton, WI) coupled by a quartz bifurcated fiber optic to the microscope epilluminator. Emission maximum at 510 nm was measured by photon counting. Data were collected from small groups of myocytes (~ 10–20 cells) using a 40× lens. Control myocytes exhibited a contraction rate of 80–100 spontaneous contractions per minute. The changes in $[Ca^{2+}]_i$ were resolved by alternating the appropriate excitation signals with a 10-segment chopper wheel at a rate of 40 revolutions per second. Background measurements at 340 and 380 nm were obtained from a sample not incubated with fura 2/AM and were automatically subtracted from acquisitions obtained from fura-2-loaded myocytes.

The experimental protocols were performed by superfusing the test solutions through the Sykes-Moore chamber at a rate of 1 ml/min. Fura 2 emission maxima were recorded using a Nikon 40× Fluor objective from groups of simultaneously contracting myocytes at prescribed time intervals during the course of the experiments. Calibration of fura 2 fluorescence was performed in the cells containing fura-2 as recommended by Scanlon et al. (20) and Peeters et al. (21). R_{max} was determined at the end of an experimental protocol by treating the cells with the nonfluorescent ionophore, 4-bromo-A23187 (20 μM) (Calbiochem-Behring Corp.) and R_{min} was determined by treatment with 5.0 mM EGTA (21). $[Ca^{2+}]_i$ was calculated according to the formula of Grynkiewicz et al. using a K_d of 225 nM (18). A series of cellular calibrations (n = 7) yielded R_{max} of 4.5±0.16, R_{min} of 0.46±0.03 and Sf2/Sb2 of 5.4±0.30. The range of fura-2 ratios was similar to that obtained with other microscope systems (22, 23).

EPMA of subcellular elemental levels. For these experiments, the culture dishes were coated with collagen gel (Collagen Corporation, Palo Alto, CA; 2.5 ml per 60-mm culture plate), forming a 1–2-mm-thick layer as previously described (10). Addition of a suspension of cells resulted in light colonization of the gels. 3 d later, media with unattached cells were removed and a second seeding of cells was added. An additional 3–4 d were required for the cells to form beating colonies of myocytes. At that point, experiments were performed as described above. At the end of the experiments, a rectangle of collagen with a cluster of beating myocytes was cut free and moved onto filter paper (Millipore Corp., Milford, MA). The filter paper-collagen-myocyte preparation was snap frozen using a cryosnapper (Model 669; Gatan Corp., Pleasanton, CA) freezing device with a pair of copper blocks cooled to liquid nitrogen temperature (−196°C) (10, 24). Cryosections were cut at a thickness of ~ 150 nm using a ultramicrotome (model MT5000) with a cryosectioning attachment (model FS1000; both obtained from DuPont, Wilmington, DE). The sections were transferred to the analytical electron microscope using a cryotransfer stage device (model 626; Gatan Corp., Pleasanton, CA). Preparations were freeze dried under vacuum in the electron microscope (24).

X-ray spectra were obtained and processed using a JEOL 1200 EX microscope (JEOL Inc., Bedford, MA and Tracor Northern). For analysis, the microscope was operated in the scanning transmission mode (STEM) at 120 kV, 30-degree specimen tilt, beam diameter of 20–60 nm, and beam current of 3 nA. The freeze-dried sections were maintained at −80°C during analysis. Scanning transmission electron micrographs of the freeze-dried cryosections also were obtained. Areas of interest were analyzed using the selected area raster mode, scan speed of 10 s per frame, and variable magnification depending upon the area of interest to be analyzed. Specifically, randomly selected areas of cytoplasm and nuclei were analyzed at a magnification of 60,000; randomly selected mitochondria were analyzed at a magnification of 200,000, such that the entire raster was filled with the mitochondrion; and small inclusions at 350,000–500,000. The x-ray spectra were collected over the range of 0 to 20 KeV for 100 s at a resolution of 10 eV per channel. Elemental peak intensities were obtained by deconvolution of the spectra using a multiple least-squares fitting technique (25). A computerized method was used for quantitative analysis of spectra,

based on the direct relationship between peak-to-continuum ratio and elemental concentration (26, 27). Spectral analysis included a computer fitting routine using the first and second derivatives of the major (K alpha) potassium peak (27). The peak-free continuum used for the calculations was from 5.5 to 7.5 KeV. Continuum counts were corrected for counts from the copper grids and from the formvar films. Peak-to-continuum ratios were converted to elemental concentrations using weighting factors derived from standard curves obtained from freeze-dried sections of gelatin-glycerol preparations containing different concentrations of various elements (25). Values obtained were for total electrolyte concentrations, including bound and free, ionized components (24–27). The data were expressed as millimoles per kilogram dry weight, with the denominator based on the local mass density derived from the continuum of the x-ray spectra (24–27).

ATP assays. ATP levels were measured by HPLC of 6% perchloric acid extracts of the cultured cells. The medium was removed from the dishes and the myocardial cells rinsed twice with a normal saline solution. The cells were removed in 1 ml of ice-cold 6% perchloric acid with 50 μM bromodeoxyuridine as internal standard, the plates washed with a second 1 ml, and the combined solutions centrifuged. The time required to extract each sample was < 25 s. Protein was collected by centrifugation, solubilized in 1 M NaOH, and measured (28). The supernatant was neutralized with 3 N KOH, filtered, and ATP measured by reverse-phase HPLC using an internal standard ratio of ATP and bromodeoxyuridine (29).

Statistical evaluation. Data were expressed as mean±SEM. Experiments involving multiple groups were evaluated by analysis of variance and Duncan's multiple range test using the Systat program or, when numbers of observations were relatively small and unequal among groups, by *t* test with Bonferroni's correction for multiple comparisons (30).

Results

Measurement of $[Ca^{2+}]_i$ *transients.* Under control conditions, neonatal cardiac myocytes exhibited rhythmic, spontaneous contractions that were associated with calcium transients (Fig. 1). In association with shortening and contraction of the myocytes, the emission produced by 340 nm excitation increased while that at 380 nm decreased, indicating an increase in $[Ca^{2+}]_i$. In association with relaxation, emission at 340 nm excitation fell while that at 380 nm increased, indicating a decrease in $[Ca^{2+}]_i$.

While being superfused with normal medium, the myocytes exhibited a contractile rate of ~ 100 bpm, with mean maximal systolic fura-2 ratios of 1.54–1.88, minimal diastolic ratios of 1.0–1.18, and maximal-minimal transient differences of 0.54–0.70 (Tables I and II). Upon exposure to media containing 1 mM ouabain, the cells ceased their contractile activity and developed contracture, and this was associated with near equalization of the systolic and diastolic fura-2 ratios at the systolic level of 1.87 after 15 min (Table I). This was followed by further increase in the fura-2 ratio to 2.71 (44% above normal systolic level), indicating increased calcium loading with continued Na^+, K^+ ATPase inhibition up to 60 min. Thereafter, the fura-2 ratio plateaued such that 120-min values were essentially the same as those recorded after 60 min. After 60 min of 1 mM ouabain treatment, return to ouabain-free superfusate resulted in a rapid decrease in $[Ca^{2+}]_i$ followed by restoration of contractile Ca^{2+} transients in all myocytes studied. After 120 min of 1 mM ouabain treatment, return to normal medium was associated with restoration of normal Ca^{2+} transients in some myocytes but persistent elevation of $[Ca^{2+}]_i$ in others.

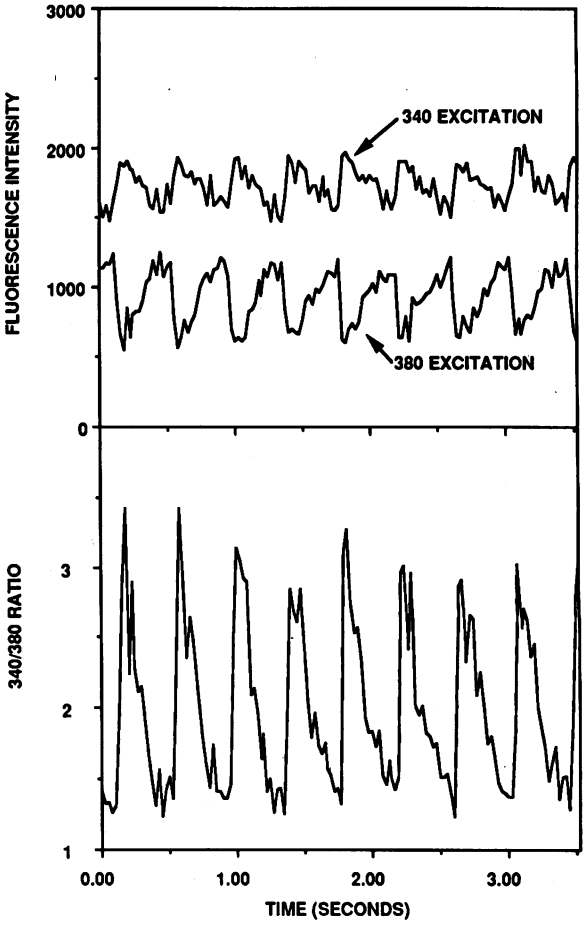

Figure 1. Dynamic microspectrofluorometric measurements from spontaneously beating cultured neonatal rat ventricular myocytes loaded with fura-2. (*Top*) Fluorescence emission intensity recording of the 340 and 380 nm excitation signals from a small group (~ 10–20 cells) of spontaneously beating myocytes. (*Bottom*) Fluorescence emission intensity ratio derived from the 340 and 380 excitation signals.

Calibrated $[Ca^{2+}]_i$ data in nM from individual experiments are presented in Figs. 2–5. Under control conditions, systolic $[Ca^{2+}]_i$ was 400–1,000 nM and diastolic $[Ca^{2+}]_i$ was 200–300 nM from the small groups of myocytes studied. As shown in Figs. 2 and 3, as the duration of Na^+, K^+ pump inhibition increased, the degree of Ca^{2+} accumulation rose to levels of 2–3 μM. Upon reexposure to ouabain-free medium after 120 min of ouabain treatment, the Ca^{2+} transients associated with contraction were restored to control levels in some myocytes, whereas other myocytes exhibited persistent elevation in $[Ca^{2+}]_i$. The level of $[Ca^{2+}]$ increase was similar in the two types of myocytes just before the recovery period.

When the myocytes were exposed to 20 mM DOG and 1 mM CN, the initial response at 15 min was a loss of normal Ca^{2+} transients associated with a decrease in $[Ca^{2+}]_i$ below the normal diastolic level (Table II). This was followed by a progressive increase in $[Ca^{2+}]$ associated with the development of contracture. After 60 min of treatment, $[Ca^{2+}]_i$ was sustained at a level intermediate between normal systolic and diastolic levels. Upon superfusion with normal medium, contractile Ca^{2+} transients were restored within 30 min (Fig. 4). Myocytes subjected to metabolic inhibition for 120 min also exhibited a

Table I. Measurements of Ionic Calcium Transients in Cultured Cardiac Myocytes after Na^+, K^+ Pump Inhibition with 1 mM Ouabain

Treatment interval (*min*)	Maximum	Fura-2 ratio (340/380) minimum	Difference
Control (*0 min*)	1.88±0.8	1.18±0.03	0.70±0.06
Ouabain (*15 min*)	1.87±0.07	1.84±0.08	0.03±0.03
Ouabain (*30 min*)	2.30±0.13	2.30±0.13	0
Ouabain (*45 min*)	2.57±0.11	2.57±0.11	0
Ouabain (*60 min*)	2.71±0.08	2.71±0.08	0
Ouabain (*60 min*) + recovery (*10 min*)	1.85±0.18	1.65±0.32	0.20±0.20
Ouabain (*60 min*) + recovery (*30 min*)	1.73±0.03	0.89±0.01	0.84±0.02
Ouabain (*90 min*)	2.60±0.07	2.60±0.07	0
Ouabain (*120 min*)	2.70±0.14	2.70±0.14	0
Ouabain (*120 min*) + recovery (*10 min*)	1.57±0.05	1.11±0.04	0.48±0.02
Ouabain (*120 min*) + recovery (*30 min*)	2.19±0.09	1.09±0.02	1.10±0.08
Ouabain (*120 min*) failed to recover at 30 min	2.45±0.13	2.45±0.13	0

Mean±SEM. n = 5–12 measurements.

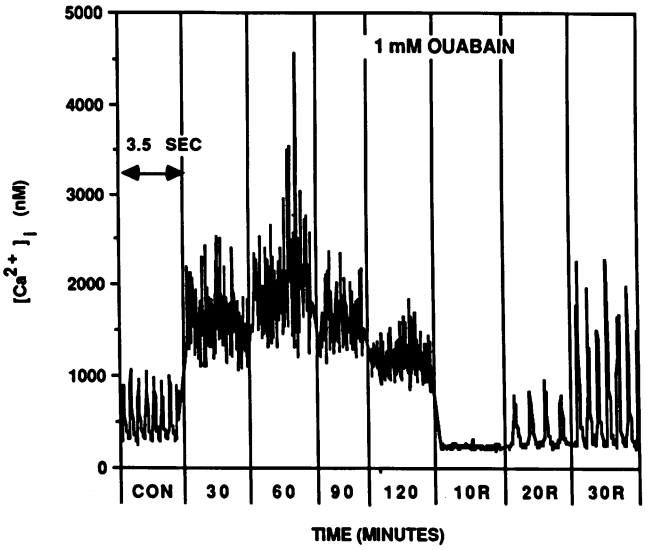

Figure 2. Individual experiment showing $[Ca^{2+}]_i$, calibrated in nanomolar, in cultured neonatal rat ventricular myocytes loaded with fura-2 and treated with 1 mM ouabain for 120 min before recovery (R) in control medium for 30 min. Each panel represents a 3.5-s interval of data recorded at the various time intervals shown on the abscissa (similar format for Figs. 3, 4, and 5). Ouabain results in loss of normal $[Ca^{2+}]_i$ transients and a sustained increase in $[Ca^{2+}]_i$. However, these myocytes show recovery of $[Ca^{2+}]_i$ transients after the period of sustained $[Ca^{2+}]_i$ increase produced by ouabain.

progressive elevation of $[Ca^{2+}]_i$ that slightly exceeded normal peak systolic level (10% increase in fura-2 ratio) by 120 min of treatment. When the myocytes were restored to normal medium, $[Ca^{2+}]_i$ in most myocytes treated for 120 min did not return to diastolic levels and contractile transients did not resume during the 30-min recovery period (Fig. 5).

Measurements of elemental contents. For EPMA studies, unstained freeze-dried cryosections were examined by STEM. Sections of control cultures exhibited well-preserved myocytes lacking distortion from freezing or specimen preparation (Fig. 6). After treatment with ouabain, cryosections exhibited numerous myocytes that contained electron dense deposits in the mitochondria (Fig. 7). In addition, there were smaller electron-dense inclusions that appeared to have an extramitochondrial location. Similar mitochondrial and extra-mitochondrial inclusions were observed in some myocytes treated

Table II. Measurements of Ionic Calcium Transients in Cultured Cardiac Myocytes after Metabolic Inhibition with 20 mM DOG and 1 mM CN

Treatment interval (*min*)	Maximum	Fura-2 ratio (340/380) minimum	Difference
Control (*0 min*)	1.54±0.06	1.00±0.08	0.54±0.04
DOG-CN (*15 min*)	0.88±0.05	0.82±0.04	0.06±0.04
DOG-CN (*30 min*)	0.86±0.04	0.86±0.04	0
DOG-CN (*45 min*)	1.16±0.09	1.16±0.09	0
DOG-CN (*60 min*)	1.27±0.11	1.27±0.11	0
DOG-CN (*60 min*) + recovery (*15 min*)	1.21±0.16	1.09±0.17	0.12±0.09
DOG-CN (*60 min*) + recovery (*30 min*)	1.31±0.07	0.81±0.04	0.50±0.05
DOG-CN (*90 min*)	1.48±0.16	1.47±0.16	0.01±0.01
DOG-CN (*120 min*)	1.70±0.14	1.70±0.14	0
DOG-CN (*120 min*) + recovery (*15 min*)	1.40±0.17	1.38±0.18	0.02±0.02
DOG-CN (*120 min*) + recovery (*30 min*)	1.41±0.19	1.41±0.19	0

Mean±SEM. n = 5–12 measurements.

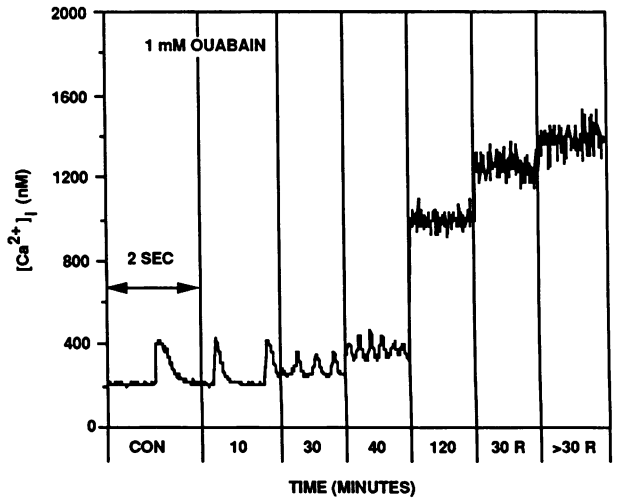

Figure 3. Individual experiment showing $[Ca^{2+}]_i$, calibrated in nanomolar, in cultured neonatal rat cardiac myocytes loaded with fura-2 and treated with 1 mM ouabain for 120 min before recovery (R) in control medium for 30 min. These myocytes exhibit a prominent increase in $[Ca^{2+}]_i$ upon exposure to ouabain and a persistent increase in $[Ca^{2+}]_i$ in the recovery period.

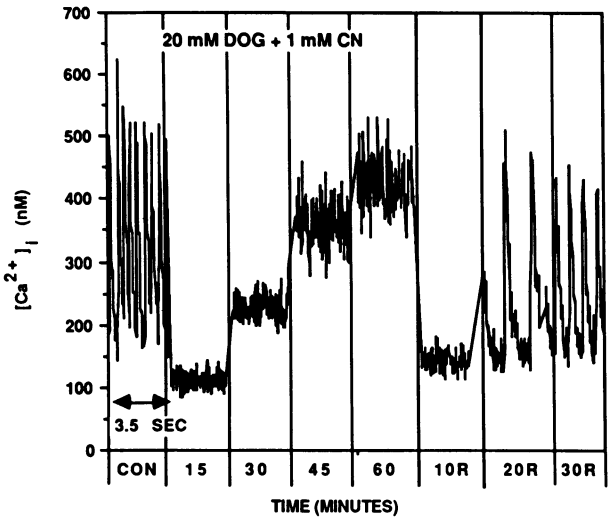

Figure 4. Individual experiment showing $[Ca^{2+}]_i$, calibrated in nanomolar, from cultured neonatal rat ventricular myocytes loaded with fura-2 and treated with 20 mM 2-deoxy-D-glucose and 1 mM sodium cyanide for 60 min before return to control medium for 30 min. Upon exposure to DOG-CN, normal $[Ca^{2+}]_i$ transients cease, and $[Ca^{2+}]_i$ initially decreases and then increases to peak systolic level. Upon return to control medium, normal $[Ca^{2+}]_i$ transients are restored.

with DOG-CN, but such inclusions were less prominent with DOG-CN than ouabain treatment.

EPMA data from cytoplasm and mitochondria are presented in Tables III and IV. Control myocytes exhibited the expected pattern of elemental concentrations with relatively high K and Mg and low Na and Ca. Elemental concentrations (expressed as millimoles per kilogram dry weight) were lower in the mitochondria than in the cytoplasm as a result of the greater mass density of the mitochondria than the cytoplasm. After 1 h of exposure to 1 mM ouabain, Na increased markedly in cytoplasm (over sevenfold) and mitochondria (over 20-fold), Cl increased significantly (1.6-fold) in the cytoplasm, K decreased significantly (60%) in both compartments, Ca increased fivefold in the cytoplasm and over 200-fold in the mitochondria, Mg decreased markedly in the cytoplasm and to a lesser degree in the mitochondria (Table III and IV). Upon return to normal medium for 30 min, myocytes showed a return to normal or nearly normal levels of all elements in the cytoplasm and mitochondria (Table III and IV). 2 h of treatment with 1 mM ouabain produced significant increases in cytoplasmic and mitochondrial Na and Ca with concurrent and equivalent decreases in K and Mg. Compared with the 1-h treatment period, cytoplasmic Ca was unchanged, but mitochondrial Ca was substantially increased. Upon return to normal medium, cytoplasmic Na and Ca showed substantial recovery, whereas cytoplasmic K and Mg were still depressed. In mitochondria, Na, K, and Ca showed substantial recovery (Table I).

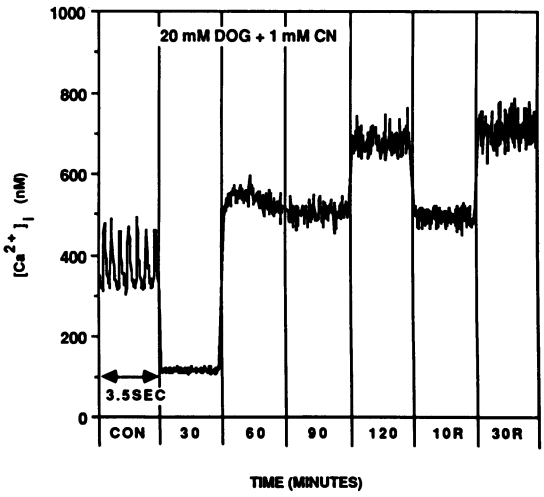

Figure 5. Individual experiment showing $[Ca^{2+}]_i$, calibrated in nanomolar, from cultured neonatal rat ventricular myocytes loaded with fura-2 and treated with 20 mM 2-deoxy-D-glucose and 1 mM sodium cyanide for 120 min before return to control medium for 30 min. DOG-CN results in an initial decrease followed by a sustained increase in $[Ca^{2+}]_i$. Upon return to control medium, there is an initial slight decrease in $[Ca^{2+}]_i$ followed by a persistent increase in $[Ca^{2+}]_i$.

After 1 h of exposure to medium containing DOG-CN, relatively mild electrolyte alterations occurred, with cytoplasmic and mitochondrial Na tending to increase and K to decrease (Tables III and IV). Cytoplasmic and mitochondrial Mg was decreased; however, total Ca was unchanged. Return to normal medium for 30 min resulted in a persistent increase in cytoplasmic and mitochondrial Na (2.5- and 5-fold) accompanied by a persistent decrease in Mg and normal K and Ca. 2 h of DOG-CN treatment produced significant increases in cytoplasmic and mitochondrial Na and significant decreases in K and Mg. Total Ca was increased in the cytoplasm and tended to increase in the mitochondria; however, the magnitude was much less than the levels produced by ouabain. Return to normal medium for 30 min resulted in substantial reduction in Na and return to normal levels of K and Ca while Mg remained significantly depressed.

Cytoplasmic and mitochondrial S in most treatment groups was decreased. Cytoplasmic P in most treatment groups was decreased, whereas mitochondrial P tended to increase in relationship to mitochondrial Ca accumulation.

ATP levels. After 1 h of treatment with 1 mM ouabain, cultures exhibited a 58% decrease in ATP content (Table V). After return to normal medium for 30 minutes, ATP content remained depressed. Cultures treated with 1 mM ouabain for 2 h also exhibited a 58% decrease, a level similar to that observed after 1 h of exposure. The ATP content remained depressed after return to normal medium for 30 min. Treatment with 20 mM DOG and 1 mM CN for 1 h produced a 70% decrease in ATP content from that of control (Table V). ATP content remained depressed at the same level after return to normal medium for 30 min. After 2 h of DOG-CN, ATP levels were reduced by 90%. After return to normal medium for 30 min, the ATP level showed partial recovery, but remained depressed at 60% of control.

Longer term recovery of metabolic homeostasis was tested by measurement of ATP content 24 h after removal of drugs and return to normal medium. At 24 h, ATP levels (percent control) were 112±14% for the 1-h ouabain group, 44.1±19% for the 2-h ouabain group, 61.1±11% for the 1-h DOG-CN group, and 55.5±8% for the 2-h DOG-CN group, respectively. Thus, there was more long-term recovery of ATP levels after 1-h treatment with ouabain than DOG-CN (P = 0.017),

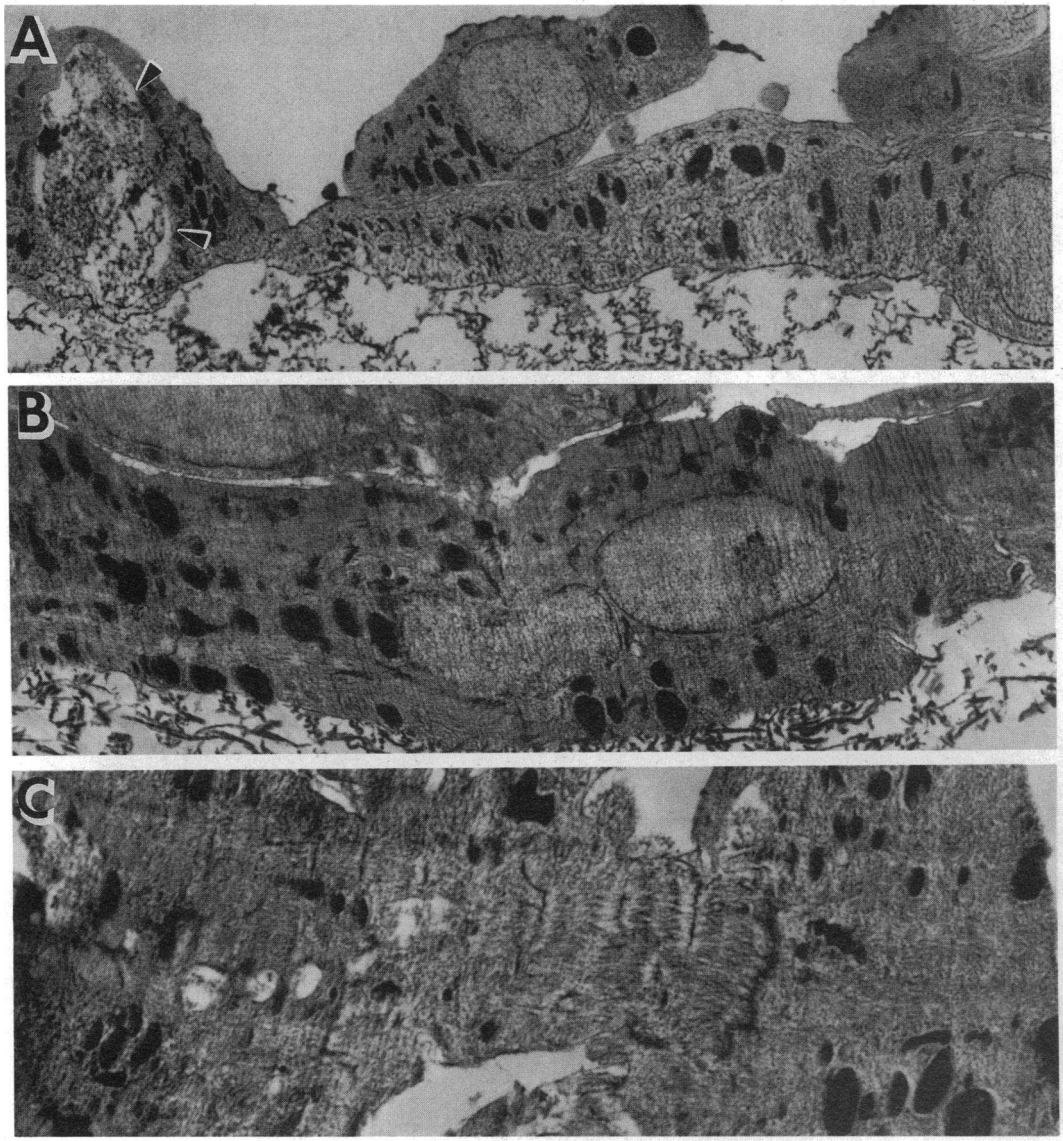

Figure 6. STEMs of freeze-dried cryosection from control cultures. The sections are unfixed and unstained; contrast is due to local mass density. (*A*) Note the superficial layer of cells on the collagen matrix. Most cells are well preserved. Cultures also typically contained a few round, edematous bodies (*arrowheads*) identified as cells that had undergone necrosis during the culture procedure. Such structures were not included in EPMA measurements. ×6,000. (*B*) Longitudinal section of a binucleate myocyte that contains dense structures with the size, shape and distribution of mitochondria. ×8,000 (*C*) Myocytes exhibit myofibrils, mitochondria, and a portion of an intercalated disc. ×16,000.

whereas long term recovery of ATP levels was depressed at a lower level after treatment for 2 h than 1 h, particularly in the ouabain groups ($P = 0.016$).

Discussion

Altered calcium homeostasis has been postulated to have an important role in the pathogenesis of irreversible myocardial ischemic injury because calcium overloading accompanies such injury in several experimental conditions (1, 5, 6, 31–33). However, it is also possible that other metabolic alterations, including impaired energy metabolism, lactate accumulation, and acidosis, may be of primary importance in the pathogenesis of irreversible injury, with calcium accumulation simply representing a secondary consequence (1–3). Indeed, the onset of irreversible myocardial injury appears to be associated with a reduction of ATP to a critical level below which essential metabolic and ionic regulatory processes can no longer be maintained (1, 2). Thus, the purpose of this study was to evaluate the relationship among calcium accumulation, ATP reduction, and the ability of cardiac myocytes to recover from these conditions.

A comprehensive analysis of calcium homeostasis was made by combining measurements obtained with a sensitive optical indicator for $[Ca^{2+}]_i$, fura-2, with EPMA measurements of total Ca and other electrolytes in subcellular compartments. By EPMA, control myocytes exhibited high K to Na and Mg to Ca ratios, and absolute Ca values, within the range reported by others (33–38). The Cl was relatively high compared with the Na, as has also been observed in other studies, suggesting active accumulation of Cl in mammalian cardiac myocytes (33–35, 38). The control $[Ca^{2+}]_i$ values were in the range for normal myocytes reported by others using various techniques including carboxylate indicators (12, 21, 39–46). In the two experimental models used, calcium loading was characterized by parallel increases in $[Ca^{2+}]_i$ and total calcium as well as by alterations in other elements, including an increase in Na and a decrease in K and Mg. EPMA showed that the mitochondria and small electron dense inclusions, possibly representing elements of sarcoplasmic reticulum,

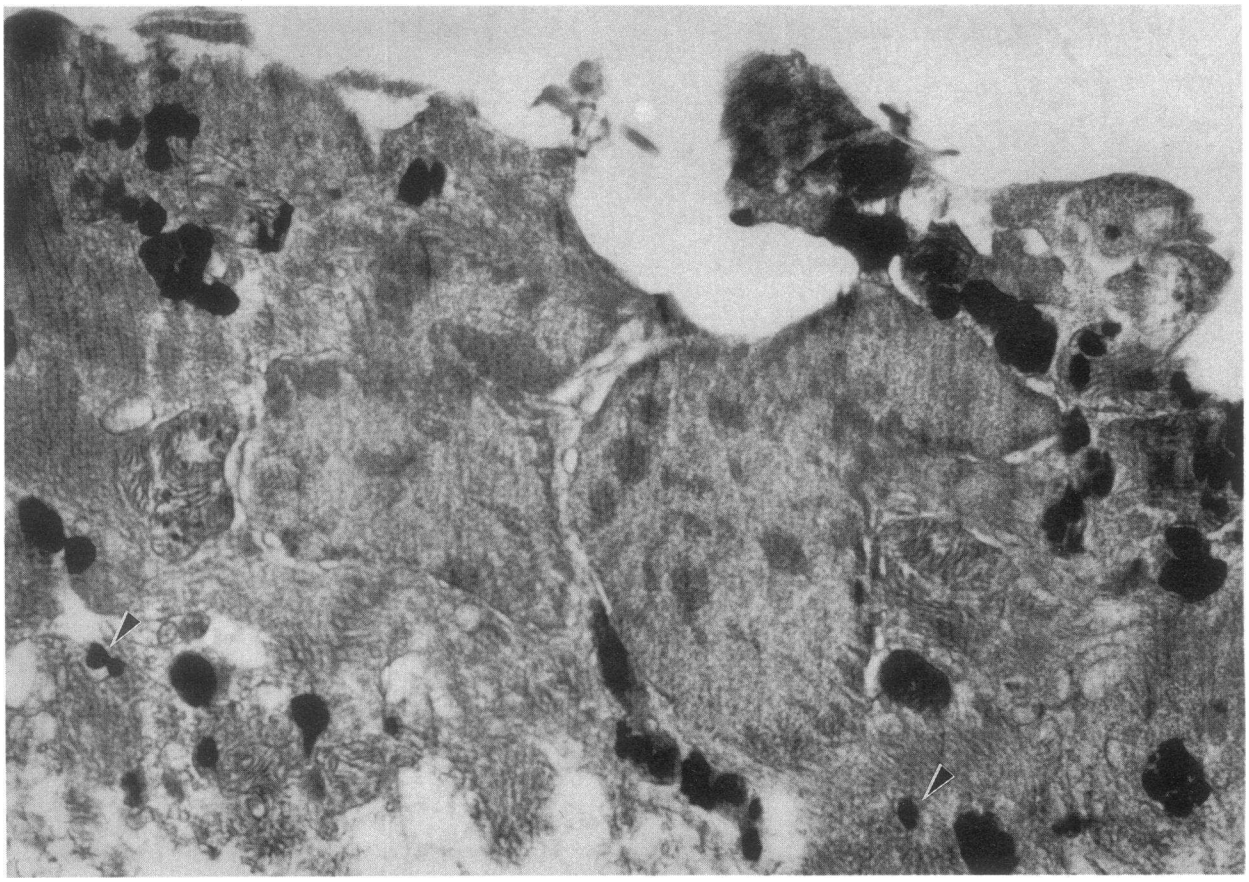

Figure 7. STEM of myocytes subjected to Na^+, K^+ pump inhibition by incubation in 1 mM ouabain for 2 h. Note the numerous electron-dense inclusions in the mitochondria, and other inclusions which appear to be extramitochondrial in location (*arrowheads*). ×17,000.

were the major sites of calcium accumulation, but that a significant increase in total calcium also occurred in the cytoplasm. These findings are consistent with the documented propensity of mitochondria and sarcoplasmic reticulum to accumulate calcium when cells are presented with an excess calcium load (1, 31, 32, 35–38). EPMA measurements also showed that the elevated calcium in the mitochondrial and extramitochondrial sites was associated with increased phosphorus, indicating the formation of calcium phosphate precipitates (10, 31, 32). It is unlikely that such precipitates contributed to the elevated fura-2 signals reflecting increased free $[Ca^{2+}]_i$ in such cells. The decreased phosphorus in the cytoplasm probably resulted from loss of inorganic phosphate from this compartment after ATP breakdown (10, 31, 32).

Na^+, K^+ pump inhibition and metabolic inhibition both produced elemental alterations; however, differences were ob-

Table III. Measurements by Electron Probe Microanalysis of Elemental Content (Millimoles/Kilogram Dry Weight) in Cytoplasm of Cardiac Myocytes under Control Conditions and after Treatment with 1 mM Ouabain or 20 mM DOG and 1 mM CN

Group	*n*	Na	Mg	P	S	Cl	K	Ca
Control	41	52±6	59±3	461±13	218±9	257±13	905±31	5±1
1 h OUB	20	410±29*‡§	9±3*‡§	360±25*§	211±17‡§	416±22*‡§	368±36*‡§	25±6*‡§
1 h OUB + 30-min rec	19	78±7§	38±4*§	425±23‡§	164±12*§	278±16‡§	952±52§	9±2§
2 h OUB	21	409±47*§	0±4*§	300±17*§	164±80*§	406±40*‡§	372±36*§	27±4*‡§
2 h OUB + 30-min rec	21	101±8§	38±2*§	418±14§	125±6*‡§	269±9§	793±19*‡§	11±2§
1 h DOG-CN	23	107±16‡	24±2*‡§	413±17§	161±16‡§	162±19*‡	780±32*‡§	5±1‡
1 h DOG-CN + 30-min rec	20	133±16*	30±6*§	501±34‡§	195±15§	172±9*‡	1,056±66§	6±2
2 h DOG-CN	20	433±29*§	3±4*§	330±29*§	191±9	247±30‡	347±40*§	15±4*‡§
2 h DOG-CN + 30-min rec	20	107±15§	30±3*§	473±18§	193±10‡	223±21	996±38‡§	5±1§

Mean±SEM. *n* = number of myocytes; 30 min rec = 30-min recovery in normal medium. For each vertical column, by analysis of variance ($P < 0.05$) and Duncan's multiple range test, * different from control, ‡ difference between ouabain and DOG-CN at same time interval, § difference between treatment and recovery.

Table IV. Measurements by Electron Probe Microanalysis of Elemental Content (Millimoles/Kilogram Dry Weight) in Mitochondria of Cardiac Myocytes under Control Conditions and after Treatment with 1 mM Ouabain or 20 mM DOG and 1 mM CN

Group	*n*	Na	Mg	P	S	Cl	K	Ca
Control	41	6±2	32±3	394±6	211±4	68±10	395±29	1±0.3
1 h OUB	20	122±9*‡§	27±3‡	450±32‡	155±7*§	84±5‡	154±18*‡§	249±69*‡§
1 h OUB + 30-min rec	20	3±2‡§	33±2‡	384±13	180±6*§	56±2	398±13§	2±1§
2 h OUB	21	94±11*‡§	47±70*‡	677±58*‡§	128±7*‡§	75±9‡	156±16*§	670±11*‡§
2 h OUB + 30-min rec	21	23±8§	42±5*‡	425±17§	155±40*‡§	66±8	354±11§	64±19§
1 h DOG-CN	23	14±4‡	11±1*‡	344±9‡	165±6*§	34±3*‡	332±14‡	1±0.4‡
1 h DOG-CN + 30-min rec	20	34±10*‡	11±1*‡	333±8	187±6*§	48±8	378±15	2±4
2 h DOG-CN	20	187±17*‡§	3±3*‡	346±33‡	169±7*‡§	116±21*‡§	159±18*§	84±49‡
2 h DOG-CN + 30-min rec	20	20±6§	13±1*‡	368±12	186±7*‡§	54±7§	378±12§	2±1

Mean±SEM. *n* = number of myocytes; 30-min rec = 30-min recovery in normal medium. For each vertical column, by analysis of variance ($P < 0.05$) and Duncan's multiple range test, * different from control, ‡ difference between ouabain and DOG-CN at same time interval, § difference between treatment and recovery.

served between the two conditions. Na^+, K^+ pump inhibition resulted in the rapid development of significant K and Mg loss and Na and Ca loading. Cessation of Ca^{2+} transients and development of contracture with elevated $[Ca^{2+}]_i$ was documented by quantitative microspectrofluorometry within 15 min of ouabain exposure; $[Ca^{2+}]_i$ peaked at 1 h and remained elevated at 2 h. The pattern of the elemental shifts detected by EPMA was consistent with Na^+ loading and K^+ efflux following inhibition of the sarcolemmal Na^+, K^+-ATPase and subsequent Ca^{2+} accumulation due to activation of the Na^+, Ca^{2+} exchanger operating in a mode favoring Ca^{2+} influx and Na^+ efflux (14–16). The severity of the Ca^{2+} loading produced by ouabain was greater than that observed after exposure of cells to low Na^+ medium (35, 45–48). In the latter condition, myocytes develop a transient increase in cytoplasmic $[Ca^{2+}]_i$ associated with increased accumulation of Ca in junctional sarcoplasmic reticulum and sarcolemma (35, 45–48). In ouabain-treated myocytes, the ATP level decreased, probably as a result of calcium-mediated activation of ATPases and inhibition of mitochondrial oxidative phosphorylation (1, 4–6, 31, 32), however, ATP reduction stabilized at a moderate level. Despite the marked Ca^{2+} loading, myocytes were able to rapidly and completely reverse electrolyte alterations, and eventually (24 h later) develop normal ATP levels after 1 h of ouabain treatment. After 2 h of ouabain, some myocytes also were able to reverse the calcium loading sufficiently to recover normal Ca^{2+} transients. However, after 2 h, significant numbers of myocytes did not recover, as shown by maintenance of high $[Ca^{2+}]_i$, failure of electrolyte profiles, including calcium, to return completely to normal, and persistent ATP depression. These findings are in accord with our observations regarding the effects of prolonged Na^+, K^+ pump inhibition in an isolated adult rat papillary muscle preparation (49). 1 h after return to complete buffer after exposure to potassium-free buffer for 3 h, papillary muscles exhibited persistent contractile depression and persistent electrolyte alterations, including increased cytoplasmic and mitochondrial calcium in significant numbers of myocytes (49).

Table V. ATP Levels in Cultured Cardiac Myocytes after Na^+, K^+ Pump Inhibition with 1 mM Ouabain and Metabolic Inhibition with 20 mM DOG and 1 mM CN

Groups (*n* = 6–14)	ATP	
	End treatment	30-min recovery
	nmol/mg protein	
Control	35.3±5.2	35.5±4.0
Ouabain (*1 mM; 1 h*)	15.0±3.4*	13.6±2.2*
Ouabain (*1 mM; 2 h*)	15.1±2.2*§	11.7±1.9*
DOG (*20 mM*) + CN (*1 mM; 1 h*)	10.6±1.6*‡	11.3±0.8*
DOG (*20 mM*) + CN (*1 mM; 2 h*)	2.9±0.7*‡§‖	13.4±2.8*‖

Mean±SEM. *n* = number of culture dishes. Statistical analysis by *t* test with Bonferroni's correction for multiple comparisons ($P < 0.001$), as follows: * significantly different from control; ‡ significantly different within treatment (1 vs. 2 h); § significantly different between treatments at same time point; and ‖ end treatment versus recovery.

In myocytes incubated with metabolic inhibitors, the mechanism of calcium loading involved impairment of energy metabolism eventually resulting in ATP depletion and subsequent impairment of ATP-dependent membrane ionic transport (8–10, 17, 50). The progressive ATP depletion resulted from direct inhibition of ATP synthetic pathways, with inhibition of glycolytically derived ATP potentially having the major effect on vital cell functions (8–10, 17, 50–57). In response to DOG and CN, myocytes developed Ca^{2+} accumulation more slowly and to a lesser degree than with ouabain. Others have reported the rapid development of contracture and Ca^{2+} elevation within minutes in response to DOG and CN (50, 51). Variation in the rate of onset of contracture may be related to differences in experimental preparations or to biological differences related to species and age of the cardiac myocytes. The rate and magnitude of ATP depletion also is a significant factor in the rate and magnitude of Ca^{2+} accumulation (44). Haworth et al. have shown that ATP depletion inhibits the rate of Ca^{2+} influx (44). The latter phenomenon may have been operative in our finding that, in spite of the marked reduction in ATP, the magnitude of the increase in $[Ca^{2+}]_i$ with DOG and CN was less than observed with ouabain. Recovery of normal Ca^{2+} transients occurred after 60 min of DOG and CN, but $[Ca^{2+}]_i$ remained at systolic level in most myocytes for

the 30-min recovery period after 120 min of DOG and CN. Partial recovery of ATP after 2 h of DOG and CN may have been associated with delayed recovery of normal Ca^{2+} homeostasis in some myocytes at 24 h, although this was not directly tested.

Thus, cultured cardiac myocytes are temporarily able to withstand the greater Ca^{2+} load induced by Na^+, K^+ pump inhibition versus metabolic inhibition with DOG and CN before developing persistent injury in response to both interventions. These results may have been influenced by a relatively high resistance of neonatal rat cardiac myocytes to the toxic effects of calcium, a resistance which may be related to functionally immature sarcoplasmic reticulum in spite of generally normal ionic regulation (58–62). Nevertheless, the findings suggest that factors associated with the specific mechanism of calcium loading have an important influence on the response of myocytes to an elevated calcium level. In our experiments, the status of energy metabolism was judged to be the important contributory factor. Specifically, the findings with Na^+, K^+ pump inhibition and metabolic inhibition suggest that the magnitude and duration of ATP depletion as well as calcium accumulation together importantly influence the severity of myocyte injury. Other factors, such as cellular acidosis related to ATP breakdown and lactate formation, also could contribute to myocyte injury. However, in these experiments, accumulation of hydrogen ions and lactate was minimized by the large volume of extracellular medium.

Other workers also have investigated the effects of Na^+-K^+ pump inhibition on isolated cells. Snowdowne and Borle reported that activation of Na^+-Ca^{2+} exchange in cultured renal cells by incubation in low Na^+ medium resulted in a transient increase of free Ca^{2+} without an increase in total Ca (48). Murphy et al. reported that Na^+, K^+ pump inhibition for 30–60 min in cultured embryonic chick myocytes produced by incubation with 0 mM K^+ or 10^{-4} M ouabain resulted in a 5–10-fold increase in free Ca^{2+} and total cell calcium content, but only modest (25–30%) reduction of ATP and no significant release of lactic dehydrogenase (LDH), and that the changes were reversible (11, 12). After 2.5 h of Na^+, K^+ pump inhibition, the ATP level was still only modestly (32%) reduced, but there was a twofold increase in LDH release. In contrast, myocytes treated with iodoacetate and an uncoupler of oxidative phosphorylation exhibited similar increases in calcium which were associated with marked reduction of ATP and significant, 10-fold LDH release (11, 12). Ishida et al. reported somewhat different observations in cultured embryonic chick ventricular cells exposed to various forms of metabolic inhibition and Na^+, K^+ pump inhibition for up to 6 h and then allowed to recover in serum-free medium for 24 h (13). Exposure to 20 mM DOG and 1 mM CN caused marked electrolyte changes, including a fivefold increase in total calcium (atomic absorption spectrophotometry), coincident with ATP depletion to one-tenth normal levels. This produced only slight cell injury, evidenced by increased LDH release, followed by recovery to normal of ATP, Na, and Ca levels, although a persistent reduction in K was noted. More marked ATP depletion (to one-hundredth normal values) was produced by hypoxia plus DOG and zero glucose, and was associated with much more severe cell injury manifested by LDH loss. Ouabain (1 mM) exposure resulted in a much greater Ca gain (20–30-fold), and ouabain effects were not reversible after a 15-fold or greater increase in Ca content was produced, and were associated with significant LDH release. The findings of Snowdowne and Borle (48) and Murphy et al. (11, 12) are in agreement with our observations of a marked increase in intracellular calcium after Na^+, K^+ pump inhibition and of substantial recovery after one hour of calcium loading secondary to Na^+, K^+ pump inhibition. However, our findings as well as those of Ishida et al. (13) indicate that more prolonged calcium loading of initially normal cells can result in significant numbers of damaged and irreversibly injured myocytes. A likely explanation for the selective death of certain myocytes after prolonged Na^+, K^+ pump inhibition or metabolic inhibition may be that the degree of calcium loading and ATP reduction was not uniform, and that those cells with more profound total calcium loading and ATP reduction developed irreversible injury.

This study has modeled some of the perturbations that occur in myocardial ischemic and hypoxic injury. However, in vitro studies with muscle preparations, adult myocytes and other cell types subjected to hypoxia and metabolic inhibition initially yielded conflicting results regarding intracellular calcium in these models. Initial studies did not show evidence of an early increase in Ca^{2+} before the onset of contracture or terminal cell injury (63–68). However, Snowdowne et al. reported a rapid increase in the range of 1.4- to 2-fold in free Ca^{2+} during early hypoxia in isolated adult rat myocytes and isolated kidney cells (69, 70). Barry et al. have reported an early increase in $[Ca^{2+}]_i$ in association with the development of contracture induced by metabolic inhibition of cultured chick cardiac myocytes (51). An early increase in $[Ca^{2+}]_i$ in response to metabolic inhibition in other cell types also has been reported (71). Additionally, investigators, using two different Ca^{2+} probes and related technologies, have demonstrated an increase in myocardial Ca^{2+} early in the course of ischemic injury in isolated perfused hearts (72–74).

Although these and previous studies have now established that Ca^{2+} increases early in the course of metabolic inhibition and hypoxic injury in isolated myocytes and ischemia in isolated perfused hearts, the exact role of calcium overloading in the genesis of myocardial ischemic membrane injury remains to be determined. Nevertheless, it is possible that in energy-depleted cells, an increase in cytosolic Ca^{2+} of sufficient magnitude and duration may induce a series of events leading to irreversible injury. Phospholipid degradation appears to be important in this process (7–9, 75, 76). Another issue is the functional consequence of calcium overloading of injured myocytes. Calcium loading contributes to the development of contracture in energy impaired cardiac myocytes, and recovery from contracture is possible depending upon the degree of metabolic impairment of the myocytes (49, 77–79). There also is evidence that calcium loading may contribute to the functional defect that follows transient myocardial ischemia (80, 81). Thus, the effects of calcium loading on energy deficient myocytes may range from the development of significant contractile impairment to irreversible injury depending upon the severity of metabolic impairment at the time of calcium loading.

In summary, our results suggest that in cells that are calcium loaded by Na^+, K^+ pump inhibition, the residual ATP initially is sufficient for maintenance of energy dependent processes involved in the repair of Ca^{2+}-mediated degradative reactions. However, prolonged calcium loading of normal myocytes eventually results in the development of significant

damage to a substantial number of cells. In contrast, in the presence of progressive ATP depletion, energy-dependent synthetic processes may not be able to compensate for Ca^{2+}-mediated catabolic reactions, thereby leading to cell death. Our findings indicate that loss of the ability to generate normal Ca^{2+} transients and persistent elevation of $[Ca^{2+}]_i$ at or greater than systolic level are markers of irreversible injury as manifest by long term impairment in the ability to regenerate ATP.

Acknowledgments

We gratefully acknowledge Ms. Linda Bolding for photographic reproduction of the electron micrographs and Ms. Dian Kammeyer for secretarial assistance.

This work was supported in part by National Institutes of Health (NIH) Ischemic Heart Disease Specialized Centers of Research grant HL-17669, NIH training grant HL-07360, and the Moss Heart Fund, Dallas, Texas.

References

1. Jennings, R. B., and K. A. Reimer. 1981. Lethal myocardial ischemic injury. *Am. J. Pathol.* 102:241–255.

2. Jennings, R. B., H. K. Hawkins, J. E. Lowe, M. L. Hill, S. Klotman, and K. A. Reimer. 1978. Relation between high energy phosphate and lethal injury in myocardial ischemia in the dog. *Am. J. Pathol.* 92:187–214.

3. Neely, J. R., and L. W. Grotyohann. 1984. Role of glycolytic products in damage to ischemic myocardium: dissociation of adenosine triphosphate levels and recovery of function of reperfused ischemic hearts. *Circ. Res.* 55:816–824.

4. Buja, L. M., and J. T. Willerson. 1981. Abnormalities of volume regulation and membrane integrity in myocardial tissue slices after early ischemic injury in the dog: effects of mannitol, polyethylene glycol, and propranolol. *Am. J. Pathol.* 103:79–95.

5. Nayler, W. G. 1981. The role of calcium in the ischemic myocardium. *Am. J. Pathol.* 102:262–270.

6. Farber, J. L. 1982. Membrane injury and calcium homeostasis in the pathogenesis of coagulation necrosis. *Lab. Invest.* 47:114–123.

7. Chien, K. R., A. Han, A. Sen, L. M. Buja, and J. T. Willerson. 1984. Accumulation of unesterified arachidonic acid in ischemic canine myocardium: relationship to a phosphatidylcholine deacylation-reacylation cycle and depletion of membrane phospholipids. *Circ. Res.* 54:313–322.

8. Chien, K. R., A. Sen, R. C. Reynolds, A. Chang, Y. Kim, M. D. Gunn, L. M. Buja, and J. T. Willerson. 1985. Release of arachidonate from membrane phospholipids in cultured neonatal rat myocardial cells during adenosine triphosphate depletion. *J. Clin. Invest.* 75:1770–1780.

9. Gunn, M. D., A. Sen, A. Chang, J. T. Willerson, L. M. Buja, and K. R. Chien. 1985. Mechanisms of accumulation of arachidonic acid in cultured myocardial cells during ATP depletion. *Am. J. Physiol.* 249:H1188–H1194.

10. Buja, L. M., H. K. Hagler, D. Parsons, K. Chien, R. C. Reynolds, and J. T. Willerson. 1985. Alterations of ultrastructure and elemental composition in cultured neonatal rat cardiac myocytes after metabolic inhibition with iodoacetic acid. *Lab. Invest.* 53:397–412.

11. Murphy, E., J. F. Aiton, C. R. Hones, and M. Lieberman. 1983. Calcium elevation in cultured heart cells: its role in cell injury. *Am. J. Physiol.* 245:C316–C321.

12. Murphy, E., R. Jacob, and M. Lieberman. 1985. Cytosolic free calcium in chick heart cells: its role in cell injury. *J. Mol. Cell. Cardiol.* 17:221–231.

13. Ishida, H., O. Kohmoto, J. H. B. Bridge, and W. H. Barry. 1988. Alterations in cation homeostasis in cultured chick ventricular cells during and after recovery from adenosine triphosphate depletion. *J. Clin. Invest.* 81:1173–1181.

14. Sutko, J. L., and J. L. Kenyon. 1983. Ryanodine modification of cardiac muscle responses to potassium-free solutions. Evidence for inhibition of sarcoplasmic reticulum calcium release. *J. Gen. Physiol.* 82:385–404.

15. Eisner, D. A. 1986. The Na-K pump in cardiac muscle. *In* The Heart and Cardiovascular System: Scientific Foundations. H. A. Fozzard, E. Haber, R. B. Jennings, A. M. Katz, and H. E. Morgan, editors, Raven Press, New York. 489–508.

16. Sheu, S. S., and M. P. Blaustein. 1986. Sodium/calcium exchange and regulation of cell calcium and contractility in cardiac muscle, with a note about vascular smooth muscle. *In* The Heart and Cardiovascular System: Scientific Foundations. H. A. Fozzard, E. Haber, R. B. Jennings, A. M. Katz, and H. E. Morgan, editors. Raven Press, New York. 509–536.

17. Webb, J. L. 1966. Enzyme and Metabolic Inhibitors. Vol. III. Academic Press, Inc., New York. 1–283.

18. Grynkiewicz, G., M. Poenie, and R. Y. Tsien. 1985. A new generation of Ca^{2+} indicators with greatly improved fluorescence properties. *J. Biol. Chem.* 260:3440–3450.

19. Vincent, R., and D. Nadeau. 1984. Adjustment of the osmolaity of Percoll for the isopycnic separation of cells and cell organelles. *Anal. Biochem.* 141:322–328.

20. Scanlon, M., D. A. Williams, and F. S. Fay. 1987. A Ca^{2+}-insensitive form of fura-2 associated with polymorphonuclear leukocytes: assessment and accurate Ca^{2+} measurement. *J. Biol. Chem.* 262:6308–6312.

21. Peeters, G. A., V. Hlady, J. H. B. Bridge, and W. H. Barry. 1987. Simultaneous measurement of calcium transients and motion in cultured heart cells. *Am. J. Physiol.* 253:H1400–H1408.

22. Poenie, M., J. Alderton, R. Y. Tsien, and R. A. Steinhardt. 1985. Changes of free calcium levels with stages of the cell division cycle. *Nature (Lond.).* 315:147–149.

23. Poenie, M., J. Alderton, R. Steinhardt, and R. Tsien. 1986. Calcium rises abruptly and briefly thoughout the cell at the onset of anaphase. *Science (Wash. DC).* 233:886–889.

24. Hagler, H. K., and L. M. Buja. 1986. Effect of specimen preparation and section transfer techniques on the preservation of ultrastructure, lipids and elements in cryosections. *J. Microsc. (Oxf.).* 141:311–317.

25. Hagler, H. K., L. E. Lopez, J. S. Flores, R. J. Lundswick, and L. M. Buja. 1983. Standards for quantitative energy dispersive x-ray microanalysis of biological cryosections: validation and application to studies of myocardium. *J. Microsc. (Oxf.).* 131:221–234.

26. Hall, T. A., H. Clarke-Anderson, and T. Appleton. 1973. The use of thin specimens for x-ray microanalysis in biology. *J. Microsc. (Oxf.).* 99:177–182.

27. Kitazawa, T., H. Shuman, and A. P. Somlyo. 1983. Quantitative electron probe analysis: problems and solutions. *Ultramicroscopy.* 11:251–262.

28. Lowry, O. H., N. J. Rosebrough, A. L. Farr, and R. J. Randall. 1951. Protein measurement with the Folin phenol reagent. *J. Biol. Chem.* 193:265–275.

29. Anderson, F. S., and R. C. Murphy. 1976. Isocratic separation of some purine nucleotide, nucleoside, and base metabolites from biological extracts by high pressure liquid chromatography. *J. Chromatogr.* 121:251–262.

30. Wallenstein, S., C. L. Zucker, and J. L. Fleiss. 1980. Some statistical methods useful in circulation research. *Circ. Res.* 47:1–9.

31. Hagler, H. K., L. Sherwin, and L. M. Buja. 1979. Effect of different methods of tissue preparation on mitochondrial inclusions of ischemic and infarcted canine myocardium: transmission and analytical electron microscopic study. *Lab. Invest.* 40:529–544.

32. Buja, L. M., K. P. Burton, H. K. Hagler, and J. T. Willerson. 1983. Alterations of elemental composition of individual myocytes in hypoxic rabbit myocardium: a quantitative x-ray microanalytical study. *Circulation.* 68:872–882.

33. Walsh, L. G., and J. McD. Tormey. 1988. Subcellular electro-

lyte shifts during in vitro myocardial ischemia and reperfusion. *Am. J. Physiol.* 255:H917–H928.

34. Wendt-Gallitelli, M. F., and R. Jacob. 1982. Rhythm-dependent role of different calcium stores in cardiac muscle: x-ray microanalysis. *J. Mol. Cell. Cardiol.* 14:487–492.

35. Wheeler-Clark, E. S., and J. McD. Tormey. 1987. Electron probe x-ray microanalysis of sarcolemma and junctional sarcoplasmic reticulum in rabbit papillary muscles: low sodium-induced calcium alterations. *Circ. Res.* 60:246–250.

36. Somlyo, A. P., M. Bond, and A. V. Somlyo. 1985. Calcium content of mitochondria and endoplasmic reticulum in liver frozen rapidly *in vivo*. *Nature (Lond.).* 314:622–625.

37. Somlyo, A. V., G. McClellan, H. Gonzales-Serratos, and A. P. Somlyo. 1985. Electron probe x-ray microanalysis of post-tetanic Ca^{2+} and Mg^{2+} movements across the sarcoplasmic reticulum *in situ*. *J. Biol. Chem.* 260:6801–6807.

38. Jorgensen, A. O., R. Broderick, A. P. Somlyo, and A. V. Somlyo. 1988. Two structurally distinct calcium storage sites in rat cardiac sarcoplasmic reticulum: an electron microprobe analysis study. *Circ. Res.* 63:1060–1069.

39. Blinks, J. R. 1986. Intracellular [Ca^{2+}] measurements. *In* The Heart and Cardiovascular System: Scientific Foundations. H. A. Fozzard, E. Haber, R. B. Jennings, A. M. Katz, and H. E. Morgan, editors. Raven Press, New York. 671–701.

40. Powell, T., P. E. R. Tatham, and V. M. Twist. 1984. Cytoplasmic free calcium measured by quin 2 fluorescence in isolated ventricular myocytes at rest and during potassium-depolarization. *Biochem. Biophys. Res. Commun.* 122:1012–1020.

41. Sheu, S., V. K. Sharma, and S. P. Banerjee. 1984. Measurement of cytosolic free calcium concentration in isolated rat ventricular myocytes with quin 2. *Circ. Res.* 55:830–834.

42. Lambert, M. R., J. D. Johnson, K. G. Lamka, G. P. Brierley, and R. A. Altschuld. 1986. Intracellular free Ca^{2+} and the hypercontracture of adult rat heart myocytes. *Arch. Biochem. Biophys.* 245:426–435.

43. Wier, W. G., M. B. Cannell, J. R. Berlin, E. Marban, and W. G. Lederer. 1987. Cellular and subcellular heterogeneity of $[Ca^{2+}]_i$ in single heart cells revealed by fura-2. *Science (Wash. DC.).* 235:325–327.

44. Haworth, R. A., A. B. Goknur, D. R. Hunter, J. O. Hegge, and H. A. Berkoff. 1987. Inhibition of calcium influx in isolated adult rat heart cells by ATP depletion. *Circ. Res.* 60:586–594.

45. Kim, D., E. J. Cragoe, Jr., and T. W. Smith. 1987. Relations among sodium pump inhibition, Na-Ca and Na-H exchange activities, and Ca-H interaction in cultured chick heart cells. *Circ. Res.* 60:185–193.

46. Kim, D., A. Okada, and T. W. Smith. 1987. Control of cytosolic calcium activity during low sodium exposure in cultured chick heart cells. *Circ. Res.* 61:29–41.

47. Eisner, D. A., C. H. Orchard, and D. G. Allen. 1984. Control of intracellular ionized calcium concentration by sarcolemmal and intracellular mechanisms. *J. Mol. Cell. Cardiol.* 16:137–146.

48. Snowdowne, K. W., and A. B. Borle. 1985. Effects of low extracellular sodium on cytosolic ionized calcium: Na^+-Ca^{2+} exchange as a major calcium influx pathway in kidney cells. *J. Biol. Chem.* 260:14998–15007.

49. Parsons, D., K. P. Burton, H. K. Hagler, and L. M. Buja. 1987. Contractile and elemental changes induced by calcium overload in papillary muscles. *Fed. Proc.* 46:1404. (Abstr).

50. Doorey, A. J., and W. H. Barry. 1983. The effects of inhibition of oxidative phosphorylation and glycolysis on contractility and high-energy phosphate content in cultured chick heart cells. *Circ. Res.* 53:192–201.

51. Barry, W. H., G. A. Peeters, C. A. F. Rasmussen, Jr., and M. J. Cunningham. 1987. Role of changes in $[Ca^{2+}]_i$ in energy deprivation contracture. *Circ. Res.* 61:726–734.

52. Bricknell, O. L., and L. H. Opie. 1978. Effects of substrates on tissue metabolic changes in the isolated rat heart during underperfusion and on release of lactate dehydrogenase and arrhythmias during reperfusion. *Circ. Res.* 43:102–115.

53. Bricknell, O. L., P. S. Daries, and L. H. Opie. 1981. A relationship between adenosine triphosphate, glycolysis and ischemic contracture in the isolated rat heart. *J. Mol. Cell. Cardiol.* 13:941–945.

54. Hasin, Y., and W. H. Barry. 1984. Myocardial metabolic inhibition and membrane potential, contraction, and potassium uptake. *Am. J. Physiol.* 247:H322–H329.

55. Weiss, J., and B. Hiltbrand. 1985. Functional compartmentation of glycolytic versus oxidative metabolism in isolated rabbit heart. *J. Clin. Invest.* 75:436–447.

56. Higgins, T. J. C., P. J. Bailey, and D. Allsopp. 1982. The interrelationship between cellular metabolic status and susceptibility of heart cells to attack by phospholipase. *J. Mol. Cell. Cardiol.* 14:645–654.

57. Higgins, T. J. C., and P. J. Bailey. 1983. The effects of cyanide and iodoacetate intoxication and ischemia on enzyme release from the perfused rat heart. *Biochem. Biophys. Acta.* 762:67–75.

58. Chizzonite, R. A., and R. Zak. 1981. Calcium-induced cell death: susceptibility of cardiac myocytes is age-dependent. *Science (Wash. DC).* 213:1508–1511.

59. Mahony, L., and L. R. Jones. 1986. Developmental changes in cardiac sarcoplasmic reticulum in sheep. *J. Biol. Chem.* 261:15257–15265.

60. Pegg, W., and M. Michalak. 1987. Differentiation of sarcoplasmic reticulum during cardiac myogenesis. *Am. J. Physiol.* 252:H22–H31.

61. Langer, G. A., A. J. Brady, S. T. Tan, and S. D. Serena. 1975. Correlation of the glycoside response, the force staircase, and the action potential configuration in the neonatal rat heart. *Circ. Res.* 36:744–752.

62. Langer, G. A., J. S. Frank, and L. M. Nudd. 1979. Correlation of calcium exchange, structure, and function in myocardial tissue culture. *Am. J. Physiol.* 237:H239–H246.

63. Cheung, J. Y., A. Leaf, and J. V. Bonventre. 1984. Mechanism of protection by verapamil and nifedipine from anoxic injury in isolated cardiac myocytes. *Am. J. Physiol.* 246:C323–C329.

64. Cheung, J. Y., A. Leaf, and J. V. Bonventre. 1986. Mitochondrial function and intracellular calcium in anoxic cardiac myocytes. *Am. J. Physiol.* 250:C18–C25.

65. Allen, D. G., and C. H. Orchard. 1983. Intracellular calcium concentration during hypoxia and metabolic inhibition in mammalian ventricular muscle. *J. Physiol. (Lond.).* 339:107–122.

66. Cobbold, P. H., and P. K. Bourne. 1984. Aequorin measurements of free calcium in single heart cells. *Nature (Lond.).* 312:444–446.

67. Allshire, A., H. M. Piper, K. S. Cuthbertson, and P. H. Cobbold. 1987. Cytosolic free Ca^{2+} in single rat heart cells during anoxia and reoxygenation. *Biochem. J.* 244:381–385.

68. Lemasters, J. J., J. Di Guiseppi, A. L. Nieminen, and B. Herman. 1987. Blebbing, free Ca^{2+} and mitochondrial membrane potential preceeding cell death in hepatocytes. *Nature (Lond.).* 325:78–81.

69. Snowdowne, K. W., R. J. Ertel, and A. B. Borle. 1985. Measurement of cytosolic calcium with aequorin in dispersed rat ventricular cells. *J. Mol. Cell. Cardiol.* 17:233–241.

70. Snowdowne, K. W., C. C. Freuderrich, and A. B. Borle. 1985. The effects of anoxia on cytosolic free calcium, calcium fluxes, and cellular ATP levels in cultured kidney cells. *J. Biol. Chem.* 260:11619–11626.

71. McCoy, C. E., A. M. Selvaggio, E. A. Alexander, and J. H. Schwartz. 1988. Adenosine triphosphate depletion induces a rise in cytosolic free calcium in canine renal epithelial cells. *J. Clin. Invest.* 82:1326–1332.

72. Steenbergen, C., E. Murphy, L. Levy, and R. E. London. 1987. Elevation in cytosolic free calcium concentration early in myocardial ischemia in perfused rat heart. *Circ. Res.* 60:700–707.

73. Marban, E., M. Kitakaze, H. Kusuoka, J. K. Porterfield, D. T. Yue, and V. P. Chacko. 1987. Intracellular free calcium concentration

measured with 19F NMR spectroscopy in intact ferret hearts. *Proc. Natl. Acad. Sci. USA.* 84:6005–6009.

74. Lee, H.-C., N. Smith, R. Mohabir, and W. T. Clusin. 1987. Cytosolic calcium transients from the beating mammalian heart. *Proc. Natl. Acad. Sci. USA.* 84:7793–7797.

75. Sen, A., J. C. Miller, R. Reynolds, J. T. Willerson, L. M. Buja, and K. R. Chien. 1988. Inhibition of the release of arachidonic acid prevents the development of sarcolemmal membrane defects in cultured rat myocardial cells during adenosine triphosphate depletion. *J. Clin. Invest.* 82:1333–1338.

76. Jones, R. L., J. C. Miller, P. K. Williams, K. R. Chien, J. T. Willerson, and L. M. Buja. 1987. The relationship between arachidonate release and calcium overloading during ATP depletion in cultured neonatal rat cardiac myocytes. *Fed. Proc.* 46:1152. (Abstr.)

77. Hasin, Y., A. Doorey, and W. H. Barry. 1984. Effects of calcium flux inhibitors on contracture and calcium content during inhibition of high energy phosphate production in cultured heart cells. *J. Mol. Cell. Cardiol.* 16:823–834.

78. Poole-Wilson, P. A., D. P. Harding, P. D. V. Bourdillon, and M. A. Tones. 1984. Calcium out of control. *J. Mol. Cell. Cardiol.* 16:175–187.

79. Renlund, D. G., G. Gerstenblith, E. G. Lakatta, W. E. Jacobus, C. H. Kallman, and M. L. Weisfeldt. 1984. Perfusate sodium during ischemia modifies post-ischemic functional and metabolic recovery in the rabbit heart. *J. Mol. Cell. Cardiol.* 16:795–801.

80. Bush, L. R., L. M. Buja, G. Tilton, M. Wathen, P. Apprill, J. Ashton, and J. T. Willerson. 1985. Effects of propranolol and diltiazem alone and in combination on the recovery of left ventricular segmental function after long-term reperfusion following temporary coronary occlusion in conscious dogs. *Circulation.* 72:413–430.

81. Kusuoka, H., J. K. Porterfield, H. F. Weisman, M. L. Weisfeldt, and E. Marban. 1987. Pathophysiology and pathogenesis of stunned myocardium: depressed Ca^{2+} activation of contraction as a consequence of reperfusion-induced cellular calcium overload in ferret hearts. *J. Clin. Invest.* 79:950–961.